applied mechanics

MDPI

Article

Mechanical Behavior of Thermoplastic Unidirectional-Tape-Reinforced Polycarbonate Produced by Additive Manufacturing: Experimental Analysis and Practical Numerical Modeling

Hagen Bankwitz *, Jörg Matthes and Jörg Hübler

Occupational Group Construction, Faculty of Engineering Sciences, University of Applied Sciences Mittweida, Technikumplatz 17, 09648 Mittweida, Germany
* Correspondence: bankwitz@hs-mittweida.de

Abstract

Additive Manufacturing (AM) using Fused Layer Modelling (FLM) often results in polymer components with limited and highly anisotropic mechanical properties, exhibiting structural weaknesses in the layer direction (Z-direction) due to low interlaminar adhesion. The main objective of this work was to investigate and quantify these mechanical limitations and to develop strategies for their mitigation. Specifically, this study aimed to (1) characterize the anisotropic behavior of unreinforced Polycarbonate (PC) components, (2) evaluate the effect of continuous, unidirectional (UD) carbon fiber tape reinforcement on mechanical performance, and (3) validate experimental findings through Finite Element Method (FEM) simulations to support predictive modeling of reinforced FLM structures. Methods involved experimental tensile and 3-point bending tests on specimens printed in all three spatial directions (X, Y, Z), validated against FEM simulations in ANSYS Composite PrepPost (ACP) using an orthotropic material model and the Hashin failure criterion. Results showed unreinforced samples had a pronounced anisotropy, with tensile strength reduced by over 70% in the Z direction. UD tape integration nearly eliminated this orthotropic behavior and led to strength gains of over 400% in tensile and flexural strength in the Z-direction. The FEM simulations showed very good agreement regarding initial stiffness and failure load. Targeted UD tape reinforcement effectively compensates for the weaknesses of FLM structures, although the quality of the tape–matrix bond and process reproducibility remain decisive factors for the reliability of the composite system, underscoring the necessity for targeted process optimization.

Keywords: fused layer modelling (FLM); polycarbonate (PC); unidirectional tape reinforcement; anisotropy; Hashin failure criterion

check for updates

Received: 28 October 2025
Revised: 28 November 2025
Accepted: 3 December 2025
Published: 9 December 2025

Citation: Bankwitz, H.; Matthes, J.; Hübler, J. Mechanical Behavior of Thermoplastic Unidirectional-Tape-Reinforced Polycarbonate Produced by Additive Manufacturing: Experimental Analysis and Practical Numerical Modeling. *Appl. Mech.* **2025**, *6*, 88. https://doi.org/10.3390/applmech6040088

Copyright: © 2025 by the authors. Licensee MDPI, Basel, Switzerland. This article is an open access article distributed under the terms and conditions of the Creative Commons Attribution (CC BY) license (https://creativecommons.org/licenses/by/4.0/).

1. Introduction

Additive manufacturing (AM), colloquially known as 3D printing, has developed into a transformative production technology in recent decades [1–5]. In particular, fused deposition modelling (FDM) or fused layer modelling (FLM), a material extrusion method, is characterised by its versatility, user-friendliness, flexibility and cost-efficiency [2,6–9]. This technology enables the tool-free production of three-dimensional components by depositing a molten thermoplastic strand layer by layer [7,8,10]. The main advantages include the ability to create complex geometries, the rapid conversion of digital model

data into the final product, and the possibility of component consolidation and functional integration [3,5,7,10].

Despite these advantages, the mechanical properties of pure polymer FDM components are often limited compared to conventional manufacturing processes [7,10,11]. A key factor here is the anisotropic mechanical behaviour of the components, which is exacerbated by the layer-by-layer build process [2,7,10–14]. This manifests itself in different mechanical properties along different axes and, in some cases, significantly lower strength perpendicular to the fibre direction due to the lower interfacial strength compared to the pure matrix [11,15]. Frequently occurring defects such as pores and voids, rough surfaces and poor adhesion between the layers or between the fibre and the matrix further impair the mechanical performance [2,7,11,14,16,17]. Polylactide (PLA), acrylonitrile butadiene styrene (ABS) and nylon are the most commonly used thermoplastics for FDM filaments due to their low melting temperature but are mainly used for concept or prototype models as they have low strength and functional properties in their pure form [6,7].

In order to overcome these limitations and improve mechanical properties, the reinforcement of thermoplastics with fibres is increasingly being investigated [2,7,10,15,18–21]. Fibre-reinforced plastics (FRPs) offer superior specific strength and stiffness, corrosion resistance and improved fatigue life [1,22]. While short fibre reinforcement (SFRC) can improve tensile strength and Young's modulus, it often has a negative effect on ductility, toughness and yield strength and increases the porosity of the printed component [7,21]. In contrast, continuous fibre reinforced composites (CFRCs) offer significantly higher strength and are of great importance for high-performance applications in aerospace, automotive, marine, sports equipment and medical technology [2,7,16,18,20,23]. Commonly used fibres are carbon fibres, glass fibres and aramid fibres (Kevlar) [2,7,18,20,24]. Carbon fibres dominate high-performance applications due to their superior strength-to-weight ratio and high modulus [2,18].

FLM printing systems that allow continuous fibres to be integrated into the print layer are currently available on the market. This technology significantly increases the strength and stiffness of components under pure bending stress [25]. This allows bending strengths and bending stiffnesses similar to those of aluminium alloy 6061 to be achieved in the XY direction [25].

The reinforcement achieved is limited to the pressure plane, as it is not possible to orient the continuous fibres in the Z direction during the manufacturing process. Consequently, adequate replication of three-dimensional loads is only possible to a limited extent.

A promising strategy for improving the mechanical properties and reducing the anisotropic behaviour of additively manufactured structures is the integration of continuous, unidirectional fibre tapes (UD tapes) [3,12]. UD tapes are flat tapes with embedded parallel fibres that offer excellent mechanical strength and stiffness in the longitudinal direction of the fibre [15,26]. Combining them with a fused granular fabrication (FGF) process (a form of FLM that processes granules directly) enables faster production and a wider range of usable materials, as the step of prefabricating filaments is eliminated [12,17]. This is particularly relevant for large-format additive manufacturing (LFAM) [12].

However, the effectiveness of UD tape reinforcement depends largely on the quality of the bond between the UD tape and the additively manufactured base structure [3,12]. Factors such as the surface quality of the FGF structure, the interface morphology and the parameters of the tape deposition process are crucial here [3,12]. Previous studies have shown that even with the same filament composition, different printing results can be achieved and that each parameter combination leads to different results [6]. A comprehensive visual representation of the various factors that influence the mechanical properties of FDM products is of great importance for their optimisation [6]. The mechanical

properties of continuously fibre-reinforced components depend on a variety of factors and parameters, including the choice of fibre and matrix materials and their orientation in the component [10].

Despite the growing interest in unidirectional tape reinforcement, there remains a paucity of scientific understanding of the mechanical behaviour of polycarbonate (PC) structures when reinforced with unidirectional tapes in AM processes. A paucity of systematic investigations has been identified in relation to the bonding mechanisms between PC matrices and UD tapes, the resulting interlaminar strength, and the influence of process parameters on anisotropic failure behaviour.

In this context, polycarbonate (PC) is coming into focus as a matrix material for high-performance applications. PC tapes offer excellent adhesive properties [16], which may be particularly advantageous for achieving strong interfacial bonding with UD tapes.

The central scientific problem that this study aims to address is the current lack of experimentally validated knowledge about the mechanical behaviour, failure mechanisms and interface quality of polycarbonate components reinforced with unidirectional tapes in additive manufacturing. This discrepancy in understanding hinders the reliable design, modelling and optimisation of such hybrid structures for high-performance applications.

2. Materials and Methods

2.1. Material Selection and Material Properties

Polycarbonate (PC) was chosen for the production of the samples examined—an amorphous thermoplastic with excellent impact strength, high dimensional stability and satisfactory temperature and mechanical resistance, especially in comparison to other FLM-compatible plastics [27,28]. Due to its amorphous structure, PC has a relatively uniform melt viscosity, which makes it particularly suitable for layer-by-layer construction in fused layer modelling [28]. However, in its unreinforced state, FDM-printed PC shows a significant decrease in strength in the Z direction, which is attributed to the low interlaminar adhesion between the individual layers [27,29].

Unidirectional (UD) tapes made of thermoplastic matrix material with continuous carbon fibre reinforcement were used for targeted mechanical reinforcement [30]. Commercially available UD tapes with a typical fibre volume concentration of approx. 40–60% and a thermoplastic polycarbonate matrix system were selected to ensure good compatibility with the main FLM material [31]. These tapes enable load path-oriented integration into critical component areas and offer a significantly higher specific strength and stiffness ratio than the pure polymer [32].

The mechanical characteristics of both materials, which are relevant for simulation and result interpretation, are shown in Table 1. The orthotropic material properties were taken into account for both materials (UD tape and FLM-printed PC). The data is based on manufacturer specifications [32,33].

Table 1. Mechanical properties of the materials used [32,33].

Property	Polycarbonate (FLM)	UD Tape PC-CF (Average Values)
Elastic modulus E_1 [MPa]	2307	111,000
Elastic modulus E_2 [MPa]	2307	2500
Elastic modulus E_3 [MPa]	2260	2500
Tensile strength x [MPa]	63	1560
Tensile strength y [MPa]	63	40
Tensile strength z [MPa]	42	40

The choice of this material combination allows for a targeted investigation of the reinforcement effect with identical base material and minimises interactions between the matrix and reinforcement phases. Furthermore, the use of a homogenised material model for the UD tapes and the FLM-printed PC in the FEM simulation represents an efficient approximation for the analysis of the macroscopic structural response.

Additional material parameters were required for the simulation, which are not directly available in the manufacturer's data sheets. Therefore, other sources were consulted [34,35] that address the general mechanical properties of polycarbonate (PC). The Ansys Workbench database only contains values for epoxy-based UD tapes. These were adjusted accordingly to represent the material characteristics of CF/PC UD tapes. The final parameters used are summarized in Tables 2 and 3.

Table 2. Further assumed stress limits of UD tape PC-CF.

Property	Value
Schubfestigkeit x [MPa]	60
Schubfestigkeit y [MPa]	32
Schubfestigkeit z [MPa]	60
Druckfestigkeit x [MPa]	−750
Druckfestigkeit y [MPa]	−80
Druckfestigkeit z [MPa]	−80

Table 3. Further assumed elasticity parameters of UD tape PC-CF.

Property	Value
Schubmodul xy [MPa]	4700
Schubmodul yz [MPa]	3100
Schubmodul xz [MPa]	4700
Querkontraktionszahl xy [-]	0.27
Querkontraktionszahl yz [-]	0.4
Querkontraktionszahl xz [-]	0.27

2.2. Sample Preparation and Experimental Setup

The samples were produced in two variants: as unreinforced reference samples made exclusively of polycarbonate (PC) and as UD tape-reinforced hybrid samples with specifically integrated, unidirectional carbon fibre-reinforced tapes on the surface. They were manufactured in a multi-stage process using a modified fused layer modelling (FLM) system with additional tape application. Each test was repeated five times to ensure statistical reliability.

2.2.1. FLM Production of Polycarbonate Components

An FLM printer with a heated build platform and enclosed build chamber was used for the additive manufacturing steps in order to minimise warping and delamination. The filament material consisted of technical polycarbonate with a diameter of 1.75 mm. The processing parameters were optimised based on manufacturer-recommended guidelines and preliminary tests:

- Nozzle diameter: 0.4 mm;
- Nozzle temperature: 270 °C;
- Bed temperature: 90 °C;
- Printing speed: 60 mm/s;
- Layer height: 0.08 mm;

- Infill: 100%.

The geometries of the test specimens were designed in accordance with the standards DIN EN ISO 527-2 (tensile test, type 1A) and DIN EN ISO 178 (3-point bending test) [36,37]. In order to specifically investigate the anisotropic mechanical properties resulting from the layer-by-layer structure of fused layer modelling (FLM), the specimens were manufactured in all three spatial directions (X, Y and Z directions). This allows the influence of the layers on the strength and stiffness of the components to be systematically analysed.

2.2.2. Integration of UD Tapes

Carbon fiber-reinforced UD tapes with a thermoplastic polycarbonate (PC) matrix were used for the hybrid samples. The tapes were positioned on the surface of the FLM structures in the direction of the expected tensile and flexural stresses, as these areas are subject to the highest tensile stresses. The reinforcement tapes were integrated manually after printing using external heat sources to ensure sufficient adhesion between the tape and the substrate. Manual tape placement proves to be an attractive option, especially for very small production runs, which are common in additive manufacturing, as it is quick, flexible, and economical to implement without extensive peripheral equipment.

In order to ensure the most uniform adhesion possible across all samples, standardised process parameters were defined in our experiment. Before starting the manual bonding procedure, the temperature was calibrated and maintained at a constant level across all samples. Care was taken to keep the pressure applied and the holding time as constant as possible. The tapes were applied by the same person throughout, which had a significant influence on the results described. The present methodology is supported by a large number of studies that demonstrate the crucial relevance of temperature and pressure profiles for the development of 'intimate contact' and thus for high-quality consolidation [38–40].

In addition, systematic pre-treatment of the substrate and tape was carried out, which included, for example, intensive surface cleaning and drying. The aim of this measure was to eliminate surface inhomogeneities and moisture. It is evident that such irregularities make it difficult to establish full-surface contact, especially in the early stages of consolidation [41].

After bonding under standardised conditions, all samples were visually inspected to detect defects such as air pockets, delamination or incomplete wetting. This procedure is established in the quality assurance of UD laminates, as defects at the interface can significantly influence the mechanical interface properties. In addition, each test configuration was performed with several replicates ($n = 5$) in order to statistically estimate the dispersion of the mechanical parameters due to possible manual variability [42,43].

Despite the measures implemented, certain inhomogeneities, such as different flow states of the matrix, minimal fluctuations in tape-substrate contact or slightly deviating heat conduction, cannot be completely ruled out. Such variations can manifest themselves in increased dispersion of the experimental mechanical test results, especially in samples that are tested close to their load limit. Furthermore, it should be noted that simulation models often use idealised assumptions (homogeneous material distributions, uniform interface quality), whereas real manufactured samples deviate slightly due to manufacturing tolerances.

To ensure the reproducibility of the results, identical tape lengths, widths (10 mm), positions and layers were used for all reinforced samples. This allows the effects of fibre reinforcement on the mechanical properties to be systematically compared.

Current research clearly shows that the interfacial adhesion between UD tapes and additively manufactured thermoplastic substrates is a key factor in the mechanical performance of such composite structures. The work of Fan et al. [44] demonstrates that

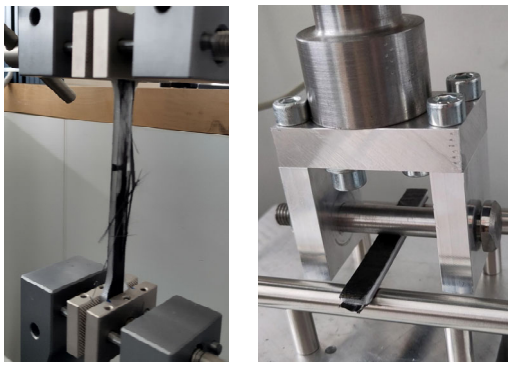
interfacial shear strength (IFSS) is significantly influenced by process parameters such as nozzle temperature, local heat distribution and material wetting. Through CT analyses, they showed that insufficient melt welding and local porosities lead to weak bonding necks, which significantly increases susceptibility to delamination. In addition, Wu et al. [45] point out that in continuously fibre-reinforced printing, especially in fused layer modelling (FLM), interface mechanics is the decisive limiting factor. They argue that even minimal defects such as microporosity, insufficient fusion or uneven compression lead to drastic losses in load transfer and therefore recommend specific test methods such as peel tests, micro-shear tests or micro-CT-based interface analyses to evaluate the composite quality.

Zhang, Chen and Yang [46] also show that fibre misalignment, fibre breakage and local waviness, as can occur during manual or semi-automated application of UD tapes, significantly weaken mechanical integrity and, in particular, flexural strength. These geometric errors lead to stress concentrations along the interface, promote the occurrence of interlaminar stresses and reduce the effective load transfer area. The experimental results of Vatandaş et al. [2] also confirm that although continuous fibres enable a significant increase in stiffness, the actual performance depends heavily on the quality of the tape-substrate bond. Inadequate process control often leads to premature delamination failure, even if the fibres themselves have high strength. Jamal et al. [38] show in a systematic parameter study that variables such as layer height, temperature control, fibre volume fraction and printing speed can either strengthen or significantly weaken the interfacial adhesion.

2.2.3. Mechanical Tests

The mechanical properties of the manufactured samples were determined by means of tensile and bending tests, with a rectangular cross-section measuring 10 mm in width and 4 mm in height.

The tensile tests were carried out in accordance with DIN EN ISO 527-2 on a universal testing machine at a test speed of 5 mm/min. The strain was measured via the crosshead travel of the testing machine. The experimental setup is shown in Figure 1a.



(**a**) (**b**)

Figure 1. Test setup: (**a**) Tensile test and (**b**) 3-point bending test.

As part of the bending test, a 3-point bending test was carried out in accordance with DIN EN ISO 178 with a span of 64 mm and a feed rate of 2 mm/min; see Figure 1b. Both the maximum deflection and the breaking load were recorded during the test. For statistical validation, at least five samples per variant were tested. In addition, the fracture surfaces were analysed to identify failure mechanisms such as delamination, fibre breakage or matrix failure.

The number of specimens (n = 5) for tensile and flexural testing is selected according to ISO 527-2 and ISO 178 standards, which recommend a minimum of five replicates per material to ensure statistically meaningful and reproducible results. This ensures that

the testing captures variation in the material behavior reliably and that the results can be statistically validated with reasonable confidence.

2.2.4. Sample Variants Examined

The three possible pressure directions initially resulted in three different variants of unreinforced samples. Each of these variants was additionally provided with a layer of UD tape, resulting in a total of six different sample types with the corresponding test geometries (tensile test and three-point bending test). All sample types were examined in both tensile and bending tests. To evaluate the repeatability and dispersion of the measurement results, each sample type was produced and tested five times. The respective printing orientations are shown in Figure 2. The green markings in the figures illustrate the primary orientation of the plastic strand deposition in the printing process. With the printing orientation T_Z_O, the test specimen is printed in the vertical Z direction.

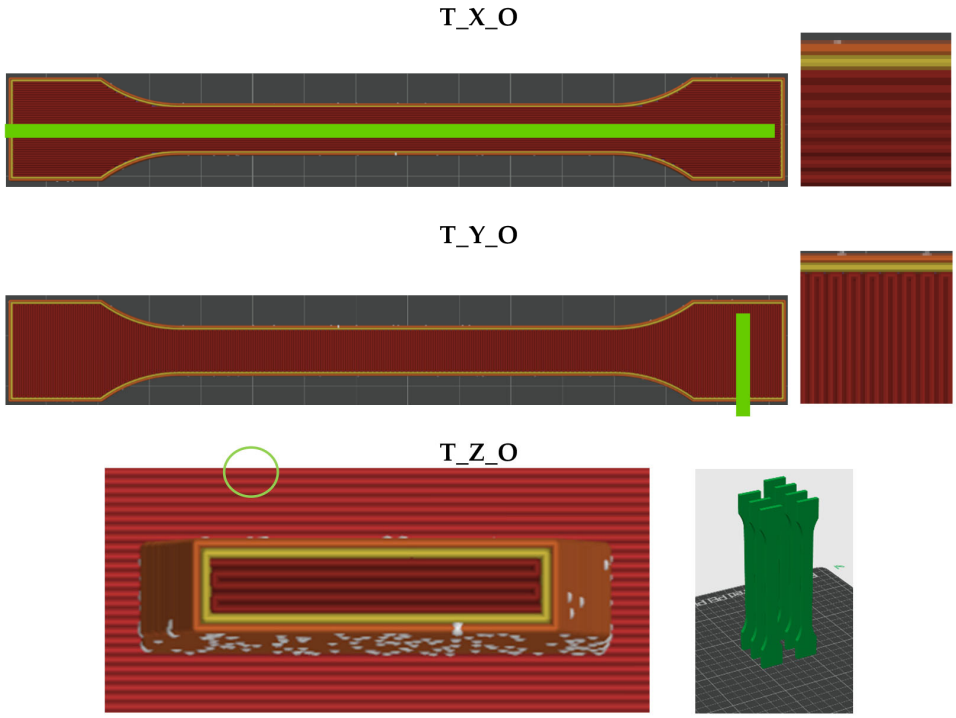


Figure 2. Print orientation of the samples, perspective from above onto the printing bed.

The names of the individual sample variants are summarised in Table 4.

Table 4. Sample designation.

Designation	Direction	Test	UD Tape Reinforcement
T_X_0	X	Tensile test	No
T_Y_0	Y	Tensile test	No
T_Z_0	Z	Tensile test	No
T_X_UD	X	Tensile test	Yes
T_Y_UD	Y	Tensile test	Yes
T_Z_UD	Z	Tensile test	Yes
B_X_0	X	Three-point bending test	No
B_Y_0	Y	Three-point bending test	No
B_Z_0	Z	Three-point bending test	No
B_X_UD	X	Three-point bending test	Yes
B_Y_UD	Y	Three-point bending test	Yes
B_Z_UD	Z	Three-point bending test	Yes

Figure 3 illustrates the program of experimental investigations.

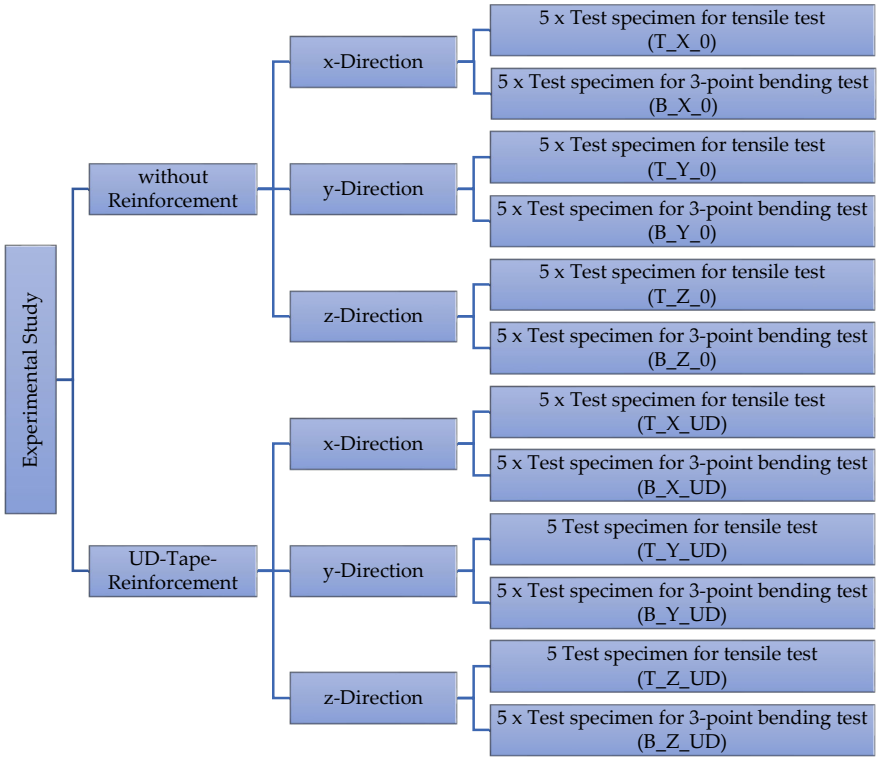


Figure 3. Program of experimental research.

2.3. Analysis of Stress States and Potential of UD Tape Reinforcement

The targeted reinforcement of polycarbonate components manufactured using fused layer modelling (FLM) with unidirectional carbon fibre-reinforced UD tapes has a significant influence on local stress conditions. The greatest advantages are apparent under tensile, compressive, bending and torsional loads, while efficiency is lower under pure shear stress.

2.3.1. Stress Distribution in Unreinforced FLM Structures

In unreinforced FLM structures, tensile and compressive stresses are distributed homogeneously across the entire cross-section under idealised conditions [47]. Under bending and torsional loads, however, the maximum normal stresses occur at the outermost surfaces [47]. In contrast, the shear stresses reach their maximum inside the component, usually in the area of the shear axis. It can be deduced that modifications close to the surface can only influence the shear capacity to a limited extent [47].

2.3.2. How UD Tape Reinforcement Works

Stresses that are highest at the surface, such as torsional and bending stresses, can be effectively reinforced with UD tapes according to their direction. It has been found that, with a homogeneous stress distribution across the cross-sectional area, reinforcement at the surface also has a significantly high effectiveness. When analysing the compressive load, however, it must be taken into account that the UD tape begins to buckle above a critical limit stress. This development can only be prevented to a limited extent by the adhesion between the tape and the component surface [47,48]. This implies that the reinforcement effect is lower than in the case of a tensile load.

Due to the significantly higher stiffness of UD tapes, modifying the surface with UD tape causes a change in the stress distribution and thus a reduction in the maximum stresses in the printed component under the same load.

2.4. Numerical Modelling

To supplement and validate the experimental results, a numerical analysis was performed using the finite element method (FEM). The aim was to map the anisotropic material behaviour and simulate failure mechanisms under tensile and bending stress under realistic boundary conditions. The simulation was performed in ANSYS Workbench 2025 R2 using the ANSYS Composite PrepPost (ACP) module, which specialises in the analysis of fibre-reinforced structures.

2.4.1. Material Modelling

A linear-elastic, orthotropic material model was used for the printed plastic. The associated parameters are listed in Table 1. This model was chosen due to the pronounced anisotropy of additively manufactured components: the mechanical properties vary depending on the direction of printing, which is particularly relevant for tensile strength. The modulus of elasticity, on the other hand, exhibits low anisotropy.

The UD tapes used were modelled as shell elements in the Ansys program using the ACP method. In this case, an orthotropic material model was used to adequately represent the highly directional mechanical properties of the continuous carbon fibres. The modelling takes into account both the high stiffness and strength in the fibre direction and the comparatively low load-bearing behaviour transverse to the fibre. The material parameters used are summarised in Table 1.

2.4.2. Geometry Model and Meshing

The geometry of the test specimens was modeled according to the actual dimensions of the tensile and flexural tests. SOLID186 hexahedral elements were used for the meshing to ensure a precise representation of the stress distribution within the layers. A refined mesh was employed in the areas of the UD tape layers to better capture local stress peaks. The bond between the FLM matrix and the UD tape was assumed to be ideally adhesive. In combination with the Hashin criterion, this approach allows for the prediction of the first crack or delamination. For the purposes of this investigation, this assumption is considered sufficient, as the structure is mechanically compromised from the moment the first damage occurs. However, actual defects cannot be accounted for in this way. These cannot be precisely determined beforehand anyway.

2.4.3. Boundary Conditions and Loading

The tests were carried out under conditions that were as close as possible to the actual test conditions. The simulations also took into account the symmetry conditions of the setup in order to reduce the mesh size.

In the tensile test, one side of the specimen (B in Figure 4) was fixed (symmetry condition), while an axial force of 3000 N was applied to the opposite side (A in Figure 4) for the unreinforced specimens and 3500 N for the specimens reinforced with UD tapes.

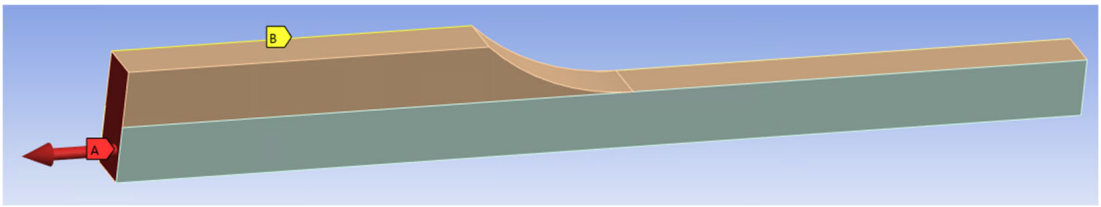


Figure 4. Model tensile test with integrated UD tape (green).

In the 3-point bending test, a support (C in Figure 5) with a defined span was set up, onto which a central vertical load (B in Figure 5) was applied by means of cylinder A in Figure 5. The load was increased quasi-statically until the preset deflection of 10 mm was reached.

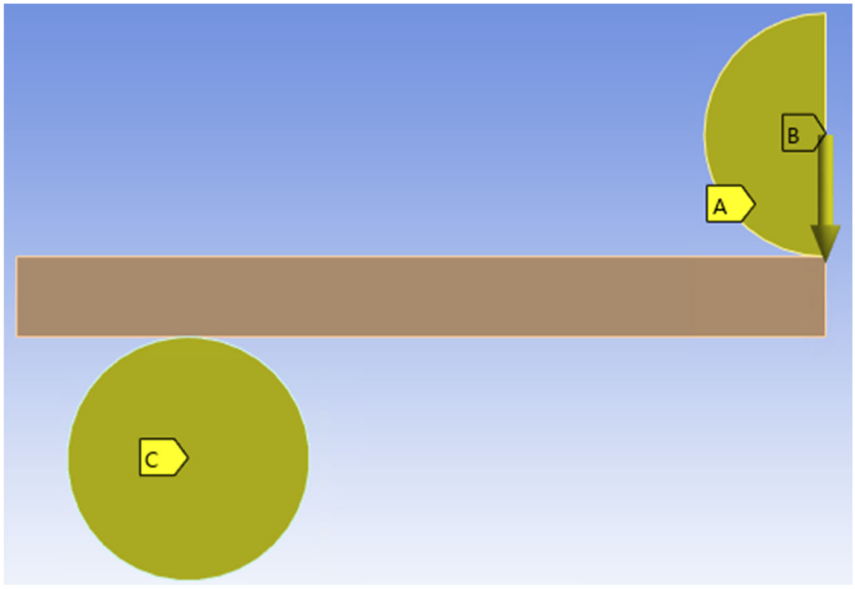


Figure 5. Model 3-point bend.

2.4.4. Failure Model for UD Tapes: Hashin Criterion

The Hashin failure criterion for unidirectional fibre-reinforced laminates was used to analyse the failure mechanisms of UD tapes [49]. The various types of damage are considered separately: fibre breakage under tension or compression, matrix failure under tension or compression, and shear failure in the plane. The Hashin criteria were implemented in ANSYS Composite PrepPost (ACP) as a progressive failure model so that the component behaviour could be simulated even after the first damage occurred. The degradation rules are based on the 'sudden drop' approach ($\alpha = 0$), in which the material properties are immediately and significantly reduced after damage occurs.

2.4.5. Validation and Correlation

The results of the FEM simulations, in particular the force–displacement and force–deflection curves, were compared with the experimental measurement data. The aim was to evaluate the model quality in terms of stiffness in the longitudinal and layer directions as well as the failure load. In addition, it was to be demonstrated that the UD tape reinforcement in specimens printed in the Z direction effectively increases the permissible strength and stiffness.

3. Results

3.1. Results of the Tensile Test

The results of the tensile tests show significant differences in mechanical behaviour between the unreinforced and UD tape-reinforced FLM polycarbonate samples. The reference samples without reinforcement (T_X_O, T_Y_O, T_Z_O; see Table 4) exhibited significant anisotropy, particularly in the Z direction (perpendicular to the layer plane). This manifested itself in greatly reduced tensile strength and lower elongation at break. In contrast, the reinforced samples exhibited a significant increase in mechanical performance.

3.1.1. Fracture Mechanics Characterization

The tensile specimens without UD-tape reinforcement generally fractured in the middle region of the sample (Figure 6, top). No influence of the printing orientation on the fracture location was observed. In contrast, several fractures in the UD-tape-reinforced specimens occurred near the clamping region, attributable to the multiaxial stress state induced by the necessary clamping force (Figure 6, bottom). Failure of the reinforced specimens was governed by fiber breakage in the UD tape.



Figure 6. Tensile fracture patterns of the specimens: top: without UD tapes; bottom: with UD tapes.

Microscopic examination was deliberately omitted, as the focus of this study was on the quantitative determination of mechanical properties, particularly tensile strength and modulus of elasticity. A detailed analysis of the fracture surfaces or microstructural defects would have required additional, time-consuming investigations beyond the defined scope of the study. However, the macroscopic measurements obtained provide sufficient information to reliably assess the mechanical performance of the samples and the effects of the UD tape reinforcement.

3.1.2. Force–Displacement Behaviour

The force–displacement curves of the unreinforced specimens in X orientation initially show linear elastic behaviour, followed by a pronounced non-linear elastic-plastic range with increasing deformation until a local maximum is reached and subsequent fracture occurs (see Figure 7). The samples in Y and Z orientation show similar behaviour, but do not reach a local maximum. Instead, fracture occurs abruptly and without prior plastic signs; see Figure 7.

In contrast, the reinforced samples show a significantly steeper rise in the force–displacement curves, indicating a higher overall modulus of elasticity. This result is consistent with the theoretical considerations regarding load absorption by the UD tapes. In addition, a minimal influence of the compressive orientation on the modulus of elasticity was observed in the reinforced samples. In a significant number of reinforced samples, initial fibre fractures are visible in the curve before failure.

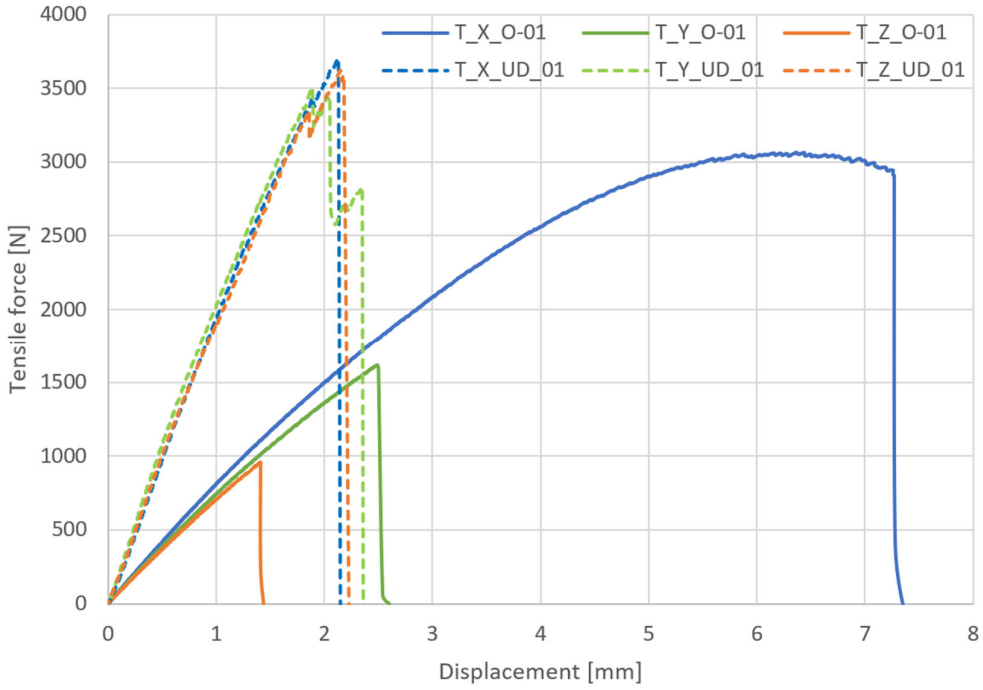


Figure 7. Force–displacement curves from the tensile test for all sample types.

3.1.3. Mechanical Characteristics

The most important averaged characteristics are summarised in Table 5. For the reinforced samples, the actual cross-section of the entire sample was taken into account when calculating the modulus of elasticity and tensile strength, with the thickness of the UD tapes included in the area determination. The values given correspond to the result averaged over the entire cross-section in order to ensure better comparability between the reinforced and unreinforced specimens.

Table 5. Overview of the results of the tensile tests.

Sample Type	(Average) Modulus of Elasticity [MPa]	(Average) Tensile Strength [MPa]	Elongation at Break [%]
T_X_O	2082 ± 23	76.9 ± 0.3	7.80 ± 0.34
T_Y_O	1966 ± 33	43.0 ± 5.0	3.07 ± 0.43
T_Z_O	1756 ± 36	22.0 ± 4.7	1.71 ± 0.23
T_X_UD	5550 ± 240	87.2 ± 5.7	3.02 ± 0.42
T_Y_UD	6018 ± 221	78.6 ± 4.3	2.56 ± 0.22
T_Z_UD	5648 ± 249	82.7 ± 6.5	2.80 ± 0.25

Furthermore, the stiffness of the test apparatus for determining the modulus of elasticity was taken into account and the measured values were corrected accordingly. The test bench stiffness k_P was 11 kN/mm.

The modulus of elasticity was calculated according to Equation (1). For this purpose, the increase $\Delta F/\Delta L$ in the initially linear range of the force–displacement curves was determined. The width b, height h and measuring length L_0 of the specimens correspond to the specifications in Section 2.2.3.

$$E = \frac{1/\left(\frac{\Delta L}{\Delta F} - 1/k_P\right) \cdot L_0}{b \cdot h} \quad (1)$$

The tensile strength was determined according to Equation (2), whereby the maximum force F_{max} was determined from the recorded force–displacement curves.

$$R_m = \frac{F_{max}}{b \cdot h} \tag{2}$$

The elongation at break was determined according to Equation (3) using the change in length ΔL at maximum force. Here too, the value is corrected for the influence of the test bench stiffness at maximum force F_{max}.

$$\varepsilon_B = \frac{\Delta L - F_{max}/k_P}{L_0} \cdot 100\% \tag{3}$$

Analysis of the unreinforced samples revealed discrepancies between the measured values and the data specified in the datasheet. The determined tensile strength significantly exceeded the specified values. This could indicate that the datasheet values were rather conservative.

A direct comparison of the measurements taken in the Y-direction with the datasheet specifications is not possible, as the definition of the Y-direction in the measurements performed differs from that in the datasheet.

Analysis of the samples in the Z-orientation revealed a reduction in the strength values and the modulus of elasticity compared to the datasheet. The cause of this phenomenon could lie in the use of a 3D printer or in differences in sample production, particularly with regard to the surface temperature during the printing process. Simultaneous production of numerous samples in a single printing process resulted in a significantly lower surface temperature. This could impair layer adhesion and consequently the mechanical properties in the Z-direction.

It is evident that the unreinforced samples exhibit clearly pronounced orthotropic behaviour in terms of their tensile strength, as is also shown in principle in the manufacturer's data sheet [33]. Under the selected printing parameters, a reduction in strength of over 70% was observed in the Z direction compared to the X direction. A significant reduction in strength of around 45% was also observed in the Y direction compared to the samples in the X direction.

The initial modulus of elasticity of all samples is in a comparable range. The modulus of elasticity of the samples in the X orientation is highest, see Table 5, while the Z-oriented samples have the lowest values, as also described in [33]. Overall, a reduction in the modulus of elasticity of around 15% was observed for the samples with Z orientation.

Accordingly, orthotropic behaviour is also evident in the elongation at break. The samples in the X orientation achieve the highest elongation at break of 7.8%, while the samples in the Z orientation exhibit the lowest elongation to failure of 1.7%, which illustrates the increased brittleness in the Z compression direction. The Y-oriented samples were relatively close to the Z-oriented samples with an elongation at break of 3.1%.

By modifying the samples with a layer of UD tape, the previously pronounced orthotropic behaviour of the printed samples was almost completely eliminated. The maximum deviation between the printing directions was only around 10%. The reason for this is the significantly higher stiffness of the UD tapes compared to the printed polycarbonate body. From a mechanical point of view, the UD tapes and the printed base body form a parallel connection of several tension springs, with the stiffer springs (UD tapes) absorbing the majority of the load in relation to their stiffness. Since the modulus of elasticity of the UD tapes is more than 43 times higher than that of printed polycarbonate, almost the entire force is transmitted via the UD tapes, which is reflected in the experimentally determined measured values.

Even with the reinforced samples, all tensile strengths are within a comparable range, but are 2.4 times higher than those of the non-reinforced samples. The reason for this is that the UD tape carries more load due to its much higher modulus of elasticity, and the tensile strength of pure UD tapes is 1560 MPa [50], which is about 25 times higher than that of FLM-printed PC.

The elongation at break of the reinforced samples showed a similar picture to that of the tensile strength. All samples are in a similar range and the influence of the print orientation of the test specimen plays a minor role.

3.2. Results of the 3-Point Bending Test

In the 3-point bending test, the FLM samples reinforced with UD tape also showed a significant increase in performance compared to the unreinforced reference samples. The integration of tape on the surface resulted, in particular, in an increase in flexural strength and stiffness. These results demonstrate the potential of targeted, load path-oriented fibre reinforcements in additively manufactured components.

3.2.1. Fracture Mechanics Characterization

Four out of five unreinforced specimens with X-orientation and one specimen with Y-orientation could not be fractured in the test setup and exhibited only plastic deformation. The remaining unreinforced specimens failed by fracture in the middle of the specimen. In contrast, all UD-tape-reinforced specimens are fractured in the central region. During testing, delamination on the compression side was observed. After the onset of delamination, the load could still be increased until final failure occurred on the tension side. Figure 8 shows an overview of the specimens after completion of the three-point bending tests.

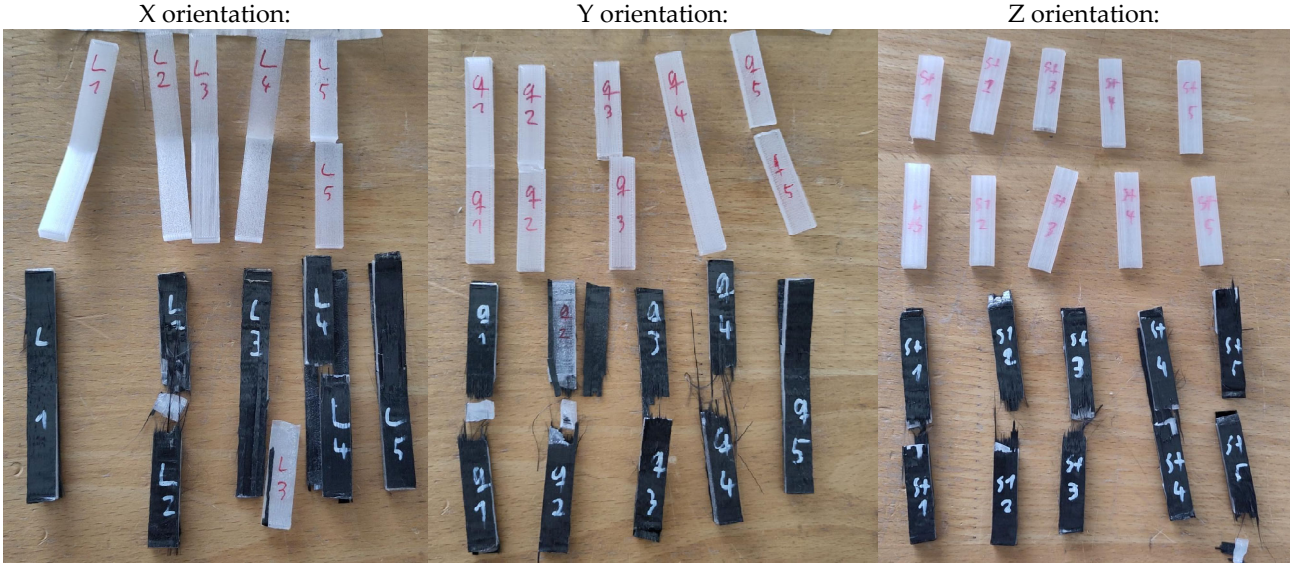


Figure 8. Fracture patterns of the specimens in the three-point bending test: top: without UD tapes; bottom: with UD tapes.

In accordance with the procedure outlined in point 3.1.1, a microscopic examination was omitted.

3.2.2. Force–Deflection Curves

The force–deflection curves of the unreinforced specimens show almost linear behaviour for small deformations; see Figure 9. With increasing deflection, non-linearity occurs, which is due to geometric changes and thus corresponds to the theoretical predictions.

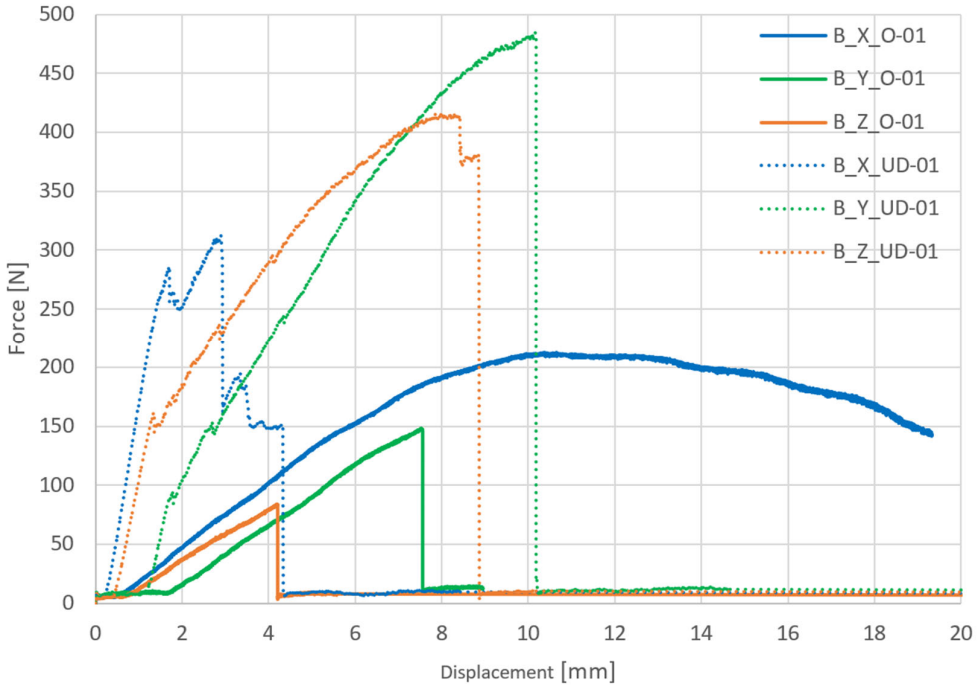


Figure 9. Force–displacement curves from the 3-point bending test for selected samples.

The evaluation of the available data shows that in the vast majority of samples with X orientation (4 out of 5), no fracture could be detected even after reaching a deflection of 20 mm (test limit); see Figure 9. In contrast, four out of five samples with Y orientation and all samples with Z orientation failed before reaching the 20 mm deflection.

The reinforced samples, on the other hand, exhibited predominantly linear-elastic behaviour up to the brittle fracture of individual fibres, which can be attributed to the dominant effect of the fibre layers. The significantly steeper rise in the force–deflection curves therefore indicates an increased flexural modulus.

In almost all cases, premature interface failure occurred in the hybrid samples at the interface between the tape and the matrix, particularly in areas of insufficient tape adhesion in the compression zone. These defects are the cause of the occasional jumps in the force–deflection curves. In addition, individual fibres on the tension side failed at an earlier stage than others, which explains the jumps in the force–displacement curve.

3.2.3. Mechanical Characteristics

The maximum deflection was derived directly from the measurement data and corresponded to the local maximum of the test cylinder's travel over the test cycle.

The average characteristic values listed in Table 6 are each based on five individual tests. The flexural strength was determined according to Equation (4), taking into account the span L and the maximum force $F_{B.max}$.

$$\sigma_{B,max} = \frac{3 \cdot F_{B.max} \cdot L}{2 \cdot b \cdot h^2} \quad (4)$$

The maximum deflection was obtained directly from the measurement data and corresponded to the local maximum of the test cylinder displacement during the test cycle.

The results show that the flexural strength of the unreinforced samples is significantly dependent on the print orientation. Samples manufactured in the Z orientation achieved only about 40% of the flexural strength of the X-oriented samples, while the Y-oriented samples had an average strength of around 80% of that of the X-oriented samples. It is also

striking that the dispersion of the measurement results for the X-oriented samples was the lowest despite the highest absolute strength values.

Table 6. Overview of the results of the three-point bending tests.

Sample Type	Bending Strength [MPa]	Maximum Deflection [mm]
B_X_O	125.6 ± 2.0	4× no break/18.3
B_Y_O	104.8 ± 13.8	1× no break/10.3 ± 4.1
B_Z_O	50.0 ± 3.1	4.1 ± 0.2
B_X_UD	164.2 ± 52.3	6.2 ± 1.6
B_Y_UD	221.7± 43.7	8.9 ± 2.4
B_Z_UD	204.4 ± 6.5	9.0 ± 1.1

This behaviour is characteristic of additively manufactured FLM components and can be explained by the anisotropic microstructure that results from the layer-by-layer application of the filaments. In the Z orientation, the interlaminar bonds between the layers act as the main load-bearing mechanism; since their strength is significantly lower than that of the polymer matrix in the strand direction, this results in a greatly reduced flexural strength. The X orientation, on the other hand, utilises the continuous strands in the direction of loading, which leads to both higher strength values and lower measurement scatter. The Y orientation represents a transitional form in which both strand orientation and layer adhesion influence the load-bearing capacity, resulting in strength values between the extremes of the X and Z orientations.

The samples reinforced with UD tape consistently exhibited increased flexural strength compared to the unreinforced samples. However, it is noticeable that the dispersion of the measured values was very large, especially for the X- and Y-oriented samples. The cause of this is believed to be manufacturing errors in the application of the UD tapes, which led to local defects or uneven adhesion. The highest flexural strength was found in the Y-oriented samples, which is probably due to the most effective adhesion between the tape and the printed body. The X-oriented samples thus exhibited strength values that were approximately 25% lower than the maximum value. The Z-oriented samples showed only a deviation of approximately 10% from the values of the Y orientation. This observation suggests that tape adhesion in this direction is less critical, as the load has a greater effect on the interlaminar layer forces.

It is also noticeable that the variance in the UD tape-reinforced samples in the X and Y orientations is relatively large. This increased dispersion is due to the manual application of the UD tapes to the printed base bodies. Manual application results in local irregularities such as wrinkles, air pockets and uneven fibre densities, which impair the adhesion between the tape and the matrix and lead to inconsistent load transfer. As a result, mechanical properties such as flexural strength can vary significantly more. The literature confirms that precise positioning and uniform compression of the UD tapes are crucial to ensure the reproducibility of the test results and to make the results comparable [51–55].

The present results lead to the conclusion that although reinforcement with UD tapes increases flexural strength in all pressure orientations, the orientation-dependent effectiveness depends significantly on the adhesion and correct application of the tape. This underlines the importance of precise manufacturing in order to consistently exploit the mechanical advantages of tape reinforcement.

The maximum deflection generally shows a positive correlation with the flexural strength in all unreinforced samples. In the X-oriented samples, only one material fracture was observed during the test, indicating high ductility in this direction. The analysis also

showed that the Y-oriented samples also exhibited high maximum deflection. In contrast, the Z-oriented samples exhibited significantly lower values.

Compared to the un-reinforced samples, the reinforced samples show higher maximum deflection with simultaneously increased flexural strengths. The values of the Y- and Z-oriented samples were at a similar level, while the X-oriented samples exhibited approximately 30% lower deflections. The results of the investigation suggest that tape reinforcement significantly increases the load-bearing capacity and, in some cases, the ductility of the samples.

3.3. Comparison of Simulation and Experiment

In the following section, selected experimental results are compared with the results of the simulation. Overall, a good agreement between simulation and experiment was achieved, especially considering the comparatively simple simulation model.

3.3.1. Tensile Test

Figure 10 shows sample test results and the corresponding simulation results without UD-tape reinforcement. The E-moduli from Table 5 were integrated to optimise the simulation. It was found that the simulation shows very good agreement with the experimental data, especially for small deformations. With increasing deformation, the specimens exhibit non-linear behaviour that cannot be represented by the linear material model of the simulation. In this case, employing a more advanced hyperelastic material model, such as the Mooney-Rivlin model, could provide a suitable solution.

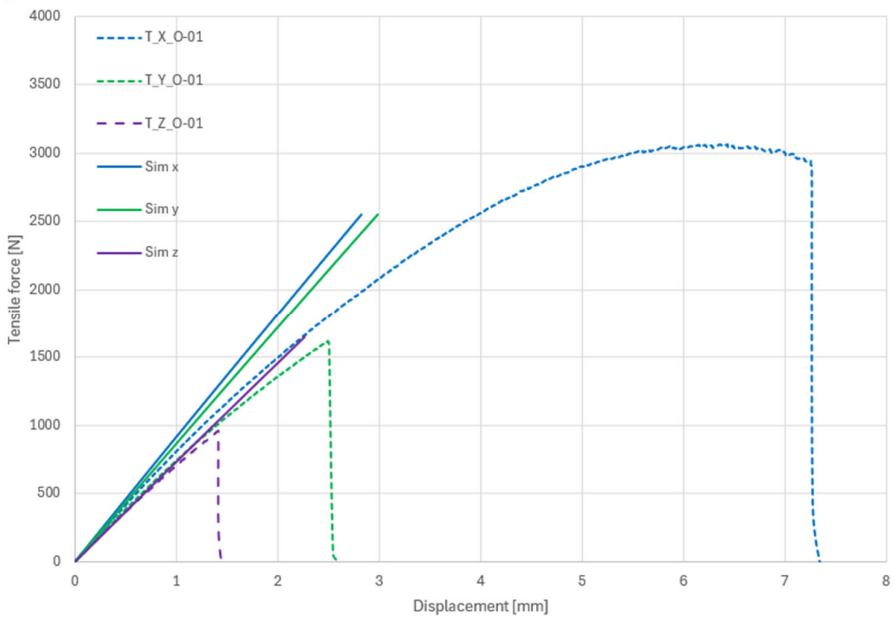


Figure 10. Force–displacement curves from tensile testing for selected unreinforced specimens and their simulations.

Table 7 shows the tensile strengths as a function of the direction of pressure for the simulation and the experimental measurements. It is striking that the tensile strength in the X direction, at around 14 MPa, is significantly higher than that specified in the data sheet. For the samples in the Y and Z directions, however, the measured values are significantly lower than the data sheet values, at around 20 MPa.

Table 7. Tensile strength simulation—measurement.

Simulation Property	Data Sheet	Measurements
Tensile strength x [MPa]	62.7	76.9 ± 0.3
Tensile strength y [MPa]	62.7	43.0 ± 5.0
Tensile strength z [MPa]	41.9	22.0 ± 4.7

For the simulation of the UD-tape-reinforced samples, only a modulus of elasticity of 2080 MPa was considered, as the stiffness of the UD tapes is several orders of magnitude higher than that of the unreinforced polycarbonate. Consequently, the modulus of the base material has only a very minor influence on the overall system. The tensile force–displacement curve shown in Figure 11 exhibits linear elastic behavior in the simulation, whereas the experimental data show a slightly nonlinear response.

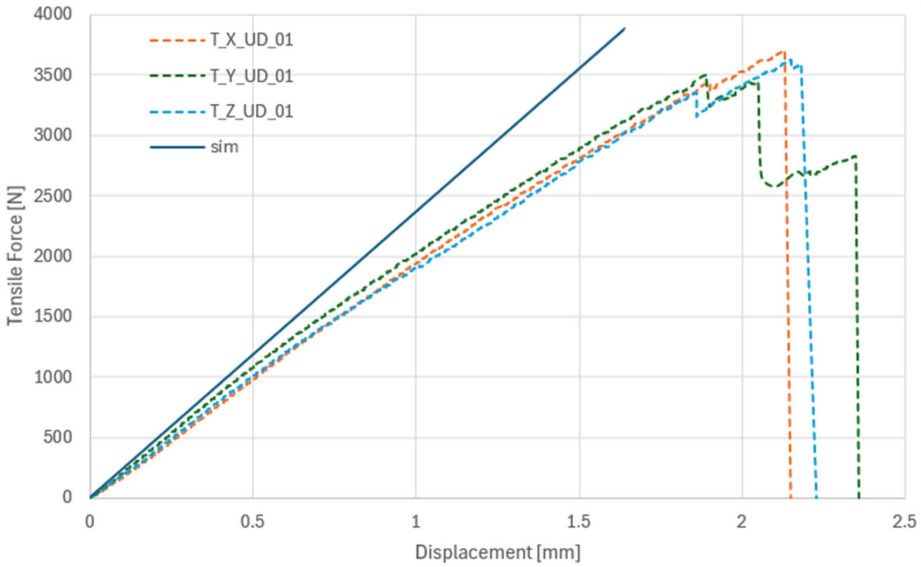


Figure 11. Force–displacement curves from tensile testing for selected reinforced samples and their simulations.

The average fracture force in the experimental investigations was approximately 3500 N. The evaluation using the Hashin criterion at this force yielded a safety factor of 1.11, corresponding to a deviation of about 11%, which indicates very good agreement with the experimental results. Fiber breakage was identified as the critical failure mode in both the simulation and the experiment.

3.3.2. Three-Point Bending Test

The simulation results for the unreinforced specimens showed very good agreement with the corresponding tests until shortly before reaching the fracture or maximum value (see Figure 12). However, with increasing deformation, the deviations between the linear material model and the experimental results increased significantly.

The bending strength determined in the simulation was lower than the measured values in all cases; see Table 8. Similarly, a lower value was determined for the maximum bending displacement in the simulation than was measured in the experimental investigations.

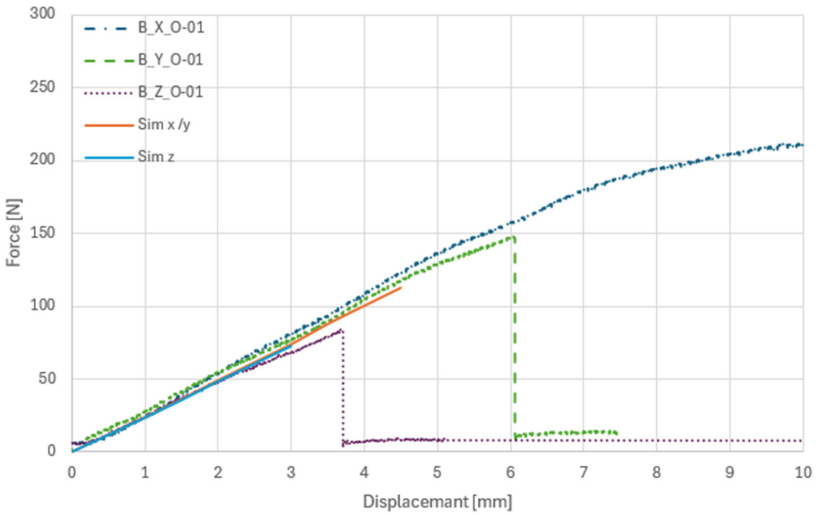


Figure 12. Force–displacement curves from the 3-point bending test for selected unreinforced specimens and their simulations.

Table 8. Flexural strength simulation—measurement.

Simulation Property	Data Sheet	Displacement [mm]	Measurements
Flexural strength x [MPa]	62.7	4.5	125.6 ± 2.0
Flexural strength y [MPa]	62.7	4.5	104.8 ± 13.8
Flexural strength z [MPa]	41.9	3	50.0 ± 3.1

The values determined in the simulation for the three-point bending showed good agreement with the experimentally measured results. However, significant stiffness jumps occurred in the measurement curves (see Figure 13), which can be attributed to partial fibre breaks within the UD tapes. This behaviour could not be captured with the simplified simulation model. In practice, however, the areas above the first fibre breaks are of minor importance, as the component is already considered damaged from this point onwards.

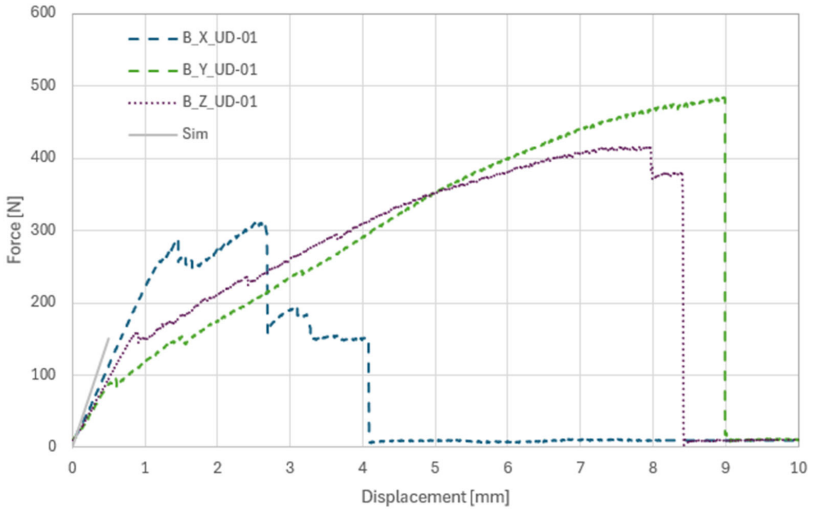


Figure 13. Force–displacement curves from the 3-point bending test for selected reinforced samples and their simulations.

With a deflection of 0.5 mm, the evaluation according to the Hashin criterion yielded a safety factor of 1.06. This shows very good agreement with the experimental results. This corresponds to a force of 150 N acting on the roller. Delamination of the pressure side was identified as the decisive failure mechanism in both the simulation and the experiment.

4. Discussion

This paper shows that the targeted integration of unidirectional, carbon fibre-reinforced UD tapes into FLM-printed polycarbonate components can significantly improve mechanical properties such as strength and stiffness. The combination of experimental validation and numerical simulation allows for a well-founded assessment of the potential and limitations of this hybrid manufacturing concept.

4.1. Effect of UD Tape Reinforcement

The experimental results demonstrate a substantial increase in stiffness and strength, particularly in the Z direction, which is a significant weak point in classic FLM structures. The load path-oriented integration of the fibre layers partially compensated for weaknesses in layer-by-layer manufacturing. The observed increases of over 400% in tensile and flexural strength, particularly in the Z-direction, underscore the effectiveness of this reinforcement strategy. At the same time, a reduction in deflection and a more brittle failure behaviour were observed, which can be attributed to the high stiffness of the fibre layers.

4.2. Limits of Tape Integration

Despite the proven advantages, the tests also revealed design and process-related challenges. In particular, the adhesion between the UD tape and the FLM matrix proved to be critical for the integrity of the composite. During bending tests on the pressure side, local delamination and buckling occurred, which, due to the nature of the process, can only be reduced by using multiple layers of tape. In addition, manual insertion of the tapes is associated with increased manufacturing tolerances, which leads to greater variation in the strength and stiffness values achieved. Targeted optimisation of the process parameters (e.g., contact pressure, temperature control, bonding strategies) therefore offers additional potential for improving composite quality.

4.3. Validity of Numerical Models

The FEM simulations with orthotropic material approach and application of the Hashin failure criterion proved to be a powerful tool for predicting the structural behaviour of the reinforced components. The high degree of agreement with the experimental results confirms the suitability of the chosen modelling strategy for UD tape-reinforced structures in 3D printing. For the unreinforced specimens, however, the simplified material model proved to be limited, as interlaminar failure mechanisms such as delamination or pore growth could not be adequately captured. However, these effects only occur at higher strains and are of minor importance for the initial stiffness and strength prediction.

4.4. Potential for Technical Applications

The combination of additive manufacturing with continuous fibre reinforcement opens up new possibilities for load-oriented lightweight construction. It should be noted that areas of application arise in particular for housings, connecting elements and structural components that are exposed to high local stresses in several spatial directions. The integration of unidirectional (UD) tapes, which are specifically aligned along the load path, offers a high degree of design freedom and leads to a significant increase in mechanical performance. In particular, types of stress that induce high surface stresses, such as bending, torsional and tensile stresses, benefit greatly from locally adapted UD tape reinforcement.

The findings obtained in this work thus form a solid basis for the further development of functionalised and mechanically optimised hybrid components in the field of additive manufacturing.

However, the scalability of the reinforcement approach examined poses a significant challenge, particularly in the case of complex geometries and larger components. The effectiveness of UD tapes depends on the structure of the material. They are most effective in simple structures with clearly defined main stress directions. In contrast, complex components often exhibit multidirectional stress conditions. Purely unidirectional reinforcement addresses these only to a limited extent. This disadvantage can be compensated for by applying several tapes in different orientations. However, it must be taken into account that this significantly increases the manufacturing effort and places high demands on the precise positioning of the reinforcement tapes.

In addition, curved or double-curved surfaces make it difficult to align the fibres without errors, as continuous tapes can only follow three-dimensional contours to a limited extent without creating defects such as wrinkles, fibre bridges or local delamination. Geometry-related irregularities can impair consolidation, reduce effective load transfer and lead to increased dispersion of mechanical characteristics.

The analysis shows that the reinforcement approach is highly suitable for simple, predominantly uniaxially loaded components, whereas its transferability to complex, multidirectionally loaded or large-format structures is limited. Further investigations and the use of automated, geometry-sensitive consolidation and tape application processes are therefore necessary for reliable scaling.

5. Conclusions

In this work, the mechanical properties of polycarbonate components manufactured using FLM technology were investigated, both with and without unidirectional (UD) carbon fiber tape reinforcement. From a scientific perspective, it was demonstrated that the integration of UD carbon fiber tapes along the load-bearing paths significantly increases mechanical performance, particularly in the otherwise weak Z-direction. To this end, systematic tensile and three-point bending tests were performed to determine the relevant parameters, which were subsequently compared with orthotropic FEM simulations in ANSYS ACP. The Hashin failure criterion proved suitable for predicting damage initiation and modeling the failure behavior of the reinforced structures. The significant agreement between experiment and simulation confirms the chosen modeling approaches for hybrid, additively manufactured fiber composite systems and underscores the scientific originality of this work.

From a practical perspective, the study demonstrated that the quality of the tape–matrix bond and the reproducibility of the manufacturing process are crucial factors for the reliability of the composite system. Local delaminations and incomplete adhesion in individual samples highlight the need for targeted process optimizations to ensure consistent mechanical performance. The results of the study support the hypothesis that hybrid additive manufacturing concepts have significant potential for producing mechanically optimized components with industrial relevance.

This opens up several perspectives for future research. Process optimization could, for example, include the implementation of automated pressing mechanisms, local preheating, or in situ control strategies to improve composite quality. The present investigation of alternative matrix materials, such as PEEK or PA6-CF, as well as variable fiber orientations, could enable application-oriented, anisotropic reinforcement. Advanced multiscale simulation approaches, including submodels or cohesive zone simulations, could contribute to optimizing the description of interlaminar failure mechanisms. Ultimately, transferring the

insights gained to components with complex geometries and practical loading scenarios—for example, in medical technology, robotics, or lightweight construction—could further demonstrate the applicability and benefits of hybrid additive manufacturing.

This work confirms that the combination of design freedom, targeted reinforcement, and digital simulation offers a promising approach for the load-dependent design of innovative, lightweight structures in industrial applications.

Author Contributions: Conceptualization, H.B. (Hagen Bankwitz), J.M. (Jörg Matthes) and J.H. (Jörg Hübler); methodology, H.B., J.M. and J.H.; software, H.B.; validation, H.B., J.M. and J.H.; formal analysis, H.B., J.M. and J.H.; investigation, H.B.; resources, H.B.; data curation, H.B.; writing—original draft preparation, H.B.; writing—review and editing, J.M. and J.H.; visualization, H.B.; supervision, H.B., J.M. and J.H.; project administration, H.B.; funding acquisition, J.M. All authors have read and agreed to the published version of the manuscript.

Funding: The authors gratefully acknowledge financial support from the Federal Ministry of Research, Technology and Space (BMFTR) through the federal-state program 'FH-Personal'.

Data Availability Statement: The original contributions presented in this study are included in the article.

Conflicts of Interest: The authors declare no conflict of interest.

Abbreviations

The following abbreviations are used in this manuscript:

B_X_O	bending specimen (B) printed in the X-direction (X) and without UD-tape reinforcement (O)
B_X_UD	bending specimen (B) printed in the X-direction (X) and reinforced with unidirectional (UD) carbon fiber tape
B_Y_O	bending specimen (B) printed in the Y-direction (Y) and without UD-tape reinforcement (O)
B_Y_UD	bending specimen (B) printed in the Y-direction (Y) and reinforced with unidirectional (UD) carbon fiber tape
B_Y_O	bending specimen (B) printed in the Z-direction (Z) and without UD-tape reinforcement (O)
B_Z_UD	bending specimen (B) printed in the Z-direction (Z) and reinforced with unidirectional (UD) carbon fiber tape
FEM	Finite Element Method
FLM	Fused Layer Modeling
T_X_0	tensile specimen (T) printed in the X-direction (X) and without UD-tape reinforcement (0 = without).
T_X_UD	tensile specimen (T) printed in the X-direction (X) and reinforced with unidirectional (UD) carbon fiber tape
T_Y_0	tensile specimen (T) printed in the Y-direction (Y) and without UD-tape reinforcement (0 = without).
T_Y_UD	tensile specimen (T) printed in the Y-direction (Y) and reinforced with unidirectional (UD) carbon fiber tape
T_Z_0	tensile specimen (T) printed in the Z-direction (Z) and without UD-tape reinforcement (0 = without).
T_Z_UD	tensile specimen (T) printed in the Z-direction (Z) and reinforced with unidirectional (UD) carbon fiber tape
UD	unidirectional

References

1. Rodriguez, P.A. Dynamic Mechanical Analysis for Quality Evaluation of Additively Manufactured Continuous Fiber Reinforced Thermoplastic Matrix Composites Subject to Manufacturing Defects. Master's Thesis, University of Nebraska, Lincoln, NE, USA, 2019.
2. Jamal, M.A.; Shah, O.R.; Ghafoor, U.; Qureshi, Y.; Bhutta, M.R. Additive Manufacturing of Continuous Fiber-Reinforced Polymer Composites via Fused Deposition Modelling: A Comprehensive Review. *Polymers* **2024**, *16*, 1622. [CrossRef] [PubMed]
3. Rackwitz, C.; Scholz, S.; Vyhnal, M.; Hirsch, P.; Schlimper, R.; Zscheyge, M.; Kotera, O.; Stipkova, M.; Scholz, S. Investigation of interfacial shear strength of hybrid fibre-reinforced polyamide composite structures made by fused granular fabrication and automated tape laying. *Prog. Addit. Manuf.* **2024**, *9*, 665–674. [CrossRef]
4. Acierno, D.; Patti, A. Fused Deposition Modelling (FDM) of Thermoplastic-Based Filaments: Process and Rheological Properties—An Overview. *Materials* **2023**, *16*, 7664. [CrossRef] [PubMed]
5. Mirza, F.; Shenoy, S.B.; Nunna, S.; Kini, C.R.; Creighton, C. Effect of material extrusion process parameters on tensile performance of pristine and discontinuous fibre reinforced PLA composites: A review. *Prog. Addit. Manuf.* **2025**, *10*, 3251–3265. [CrossRef]
6. Kristiawan, R.B.; Imaduddin, F.; Ariawan, D.; Ubaidillah, U.; Arifin, Z. A review on the fused deposition modeling (FDM) 3D printing: Filament processing, materials, and printing parameters. *Open Eng.* **2021**, *11*, 639–649. [CrossRef]
7. Wickramasinghe, S.; Do, T.; Tran, P. FDM-Based 3D Printing of Polymer and Associated Composite: A Review on Mechanical Properties, Defects and Treatments. *Polymers* **2020**, *12*, 1529. [CrossRef]
8. Raja, C.P.; Shanmugam, V.; Parrthipan, B.K.; Babu, S.; Babu, N.B.K.; Mensah, R.A. Additive manufacturing of polymers and composites for sustainable engineering applications. *Front. Chem. Eng.* **2025**, *7*, 1722765. [CrossRef]
9. Sapkota, A.; Ghimire, S.K.; Adanur, S. A review on fused deposition modeling (FDM)-based additive manufacturing (AM) methods, materials and applications for flexible fabric structures. *J. Reinf. Plast. Compos.* **2024**, *54*. [CrossRef]
10. Heitkamp, T.; Girnth, S.; Kuschmitz, S.; Klawitter, G.; Waldt, N.; Vietor, T. Continuous Fiber-Reinforced Material Extrusion with Hybrid Composites of Carbon and Aramid Fibers. *Appl. Sci.* **2022**, *12*, 8830. [CrossRef]
11. Han, Y.; Li, Z.; Wang, X. Material anisotropy in additively manufactured polymers and polymer composites: A review. *Polymers* **2021**, *13*, 3368. [CrossRef]
12. Hirsch, P.; Scholz, S.; Borowitza, B.; Vyhnal, M.; Schlimper, R.; Zscheyge, M.; Kotera, O.; Stipkova, M.; Scholz, S. Processing and Analysis of Hybrid Fiber-Reinforced Polyamide Composite Structures Made by Fused Granular Fabrication and Automated Tape Laying. *J. Manuf. Mater. Process.* **2024**, *8*, 25. [CrossRef]
13. Elli, C.; Barletta, L.; Caggiano, M. Micromechanical models for FDM 3D-printed polymers: A review. *Polymers* **2023**, *15*, 4497. [CrossRef] [PubMed]
14. Mažuranić, B. Accuracy of FDM PLA polymer 3D printing technology based on tolerance fields. *Processes* **2023**, *11*, 2810. [CrossRef]
15. Kupzik, D. Robotic Swing Folding of Three-Dimensional UD-Tape-Based Reinforcement Structures. Dissertation, Karlsruhe Institute of Technology, Karlsruhe, Germany, 2022.
16. Wang, H.H.; Huo, S.; Chevali, V.; Hall, W.; Offringa, A.; Song, P.; Wang, H. Carbon Fiber Reinforced Thermoplastics: From Materials to Manufacturing and Applications. *Adv. Mater.* **2025**, *37*, e2418709. [CrossRef]
17. Matkovic, N.; Kupzik, D.; Steidle-Sailer, C.; Friedmann, M.; Fleischer, J. Novel Robot-Based Process Chain for the Flexible Production of Thermoplastic Components with CFRP Tape Reinforcement Structures. *Procedia CIRP* **2022**, *106*, 21–26. [CrossRef]
18. Zheng, H.; Zhu, S.; Chen, L.; Wang, L.; Zhang, H.; Wang, P.; Sun, K.; Wang, H.; Liu, C. 3D Printing Continuous Fiber Reinforced Polymers: A Review of Material Selection, Process, and Mechanics-Function Integration for Targeted Applications. *Polymers* **2025**, *17*, 1601. [CrossRef]
19. Fang, G.; Zhang, T.; Zhong, S.; Chen, X.; Zhong, Z.; Wang, C.C.L. Reinforced FDM: Multi-axis filament alignment with controlled anisotropic strength. *ACM Trans. Graph.* **2020**, *39*, 1–15. [CrossRef]
20. Caminero, M.; Cano, M.; Rodríguez, M.; Pérez, P. Review of mechanical properties of and optimisation methods for continuous fibre-reinforced thermoplastic parts manufactured by fused deposition modelling. *Prog. Addit. Manuf.* **2021**, *6*, 663–677. [CrossRef]
21. Ismail, K.; Yap, C.; Ahmed, R. 3D-Printed Fiber-Reinforced Polymer Composites by Fused Deposition Modelling (FDM): Fiber Length and Fiber Implementation Techniques. *Polymers* **2022**, *14*, 4659. [CrossRef]
22. Bashir, A.; Dillon, R.P.; Callahan, J. Recent developments in improving the fracture toughness of 3D-printed fiber-reinforced polymer composites. *Compos. B Eng.* **2024**, *283*, 111622. [CrossRef]
23. Kabir, K.; Rahaman, N.; Chowdhury, B. Mechanical properties of continuous glass fibre-reinforced composites made by material extrusion. *Prog. Addit. Manuf.* **2024**, *9*, 2131–2141. [CrossRef]
24. Li, S.; Wang, K.; Zhu, W.; Peng, Y.; Ahzi, S.; Chinesta, F. Investigation on the mechanical properties of 3D printed hybrid continuous fiber-filled composite considering influence of interfaces. *Int. J. Adv. Manuf. Technol.* **2022**, *123*, 3147–3158. [CrossRef]
25. Markforged. Fiberglass—Continuous fibers. Available online: https://markforged.com/de/materials/continuous-fibers/fiberglass (accessed on 18 August 2025).

26. Fraunhofer IMWS. UD Tapes–Lightweight and high strength semi-finished products for high performance thermoplastic composites. Fraunhofer IMWS Info-Page. 2024. Available online: https://www.imws.fraunhofer.de/en/specials/ud-tapes.html (accessed on 18 August 2025).
27. Masood, S.H.; Mau, K.; Song, W.Q. Tensile properties of processed FDM polycarbonate material. *J. Mater. Process. Technol.* **2010**, *210*, 54–58. [CrossRef]
28. Materialise. Polycarbonate for Fused Deposition Modeling. Available online: https://www.materialise.com/en/industrial/3d-printing-materials/polycarbonate (accessed on 18 August 2025).
29. Einfach3Ddruck. PC Filament—Darauf solltest Du beim 3D-Druck achten! Available online: https://einfach3ddruck.de/pc-filament-im-3d-druck/ (accessed on 18 August 2025).
30. Teijin Carbon. UniDirectional Tape. Available online: https://www.teijincarbon.com/products/thermoplastics/unidirectional-tapes/ (accessed on 18 August 2025).
31. Evonik Industries. VESTAPE—Thermoplastic composites. Available online: https://tp-composites.com/wp-content/uploads/sites/3/2017/04/VESTAPE-2-2017.pdf (accessed on 18 August 2025).
32. Topolo Group. PC Resin Carbon Fiber Thermoplastic UD Tapes. Available online: https://topologroup.com/thermoplastic-prepregs/pc-resin-carbon-fiber-thermoplastic-ud-tapes/ (accessed on 18 August 2025).
33. Polymaker. PolyLite™ PC Technical Data Sheet. Version 1.2. Available online: https://3d.nice-cdn.com/upload/file/PolyLite_PC_TDS_V5.1.pdfhttps://3d.nice-cdn.com/upload/file/PolyLite_PC_TDS_V5.1.pdf (accessed on 18 August 2025).
34. Ensinger. Polycarbonate PC 1000. Ensinger Precision Components, Plastic Stock Shapes. Available online: https://www.ensinger-pc.com/injection-molding-materials/our-plastic-stock-shapes/polycarbonate-pc-1000-2 (accessed on 25 November 2025).
35. Kore, S.; Murthy, V.S.M.D.; Hiremath, N.; Theodore, M.; Young, S.; Penumadu, D.; Vaidya, U. Textile-Grade Carbon Fiber-Reinforced Polycarbonate Composites: Effect of Epoxy Sizing. *Ind. Eng. Chem. Res.* **2021**, *60*, 3981–3991. [CrossRef]
36. *DIN EN ISO 527-2:2012*; Kunststoffe—Bestimmung der Zugfestigkeit—Teil 2: Prüfungen mit Prüfkörpern in Form von Stäben. Beuth: Berlin, Germany, 2012.
37. *DIN EN ISO 178:2019*; Kunststoffe—Bestimmung der Biege-Eigenschaften. Beuth: Berlin, Germany, 2019.
38. Çelik, O.; Hosseini, S.A.; Baran, I.; Grouve, W.J.; Akkerman, R.; Peeters, D.M.; Teuwen, J.J.; Dransfeld, C.A. The influence of inter-laminar thermophysical properties on the degree of intimate contact in laser-assisted fibre placement. *Compos. A Appl. Sci. Manuf.* **2021**, *145*, 106367. [CrossRef]
39. Xiong, H.; Hamila, N.; Boisse, P. Consolidation Modeling during Thermoforming of Thermoplastic Composite Prepregs. *Materials* **2019**, *12*, 2853. [CrossRef]
40. Schaefer, P.M.; Guglhoer, T.; Sause, M.G.R.; Drechsler, K. Development of intimate contact during processing of carbon fiber reinforced Polyamide-6 tapes. *J. Reinf. Plast. Compos.* **2017**, *36*, 593–607. Available online: https://opus.bibliothek.uni-augsburg.de/opus4/60071 (accessed on 2 December 2025). [CrossRef]
41. Sacchetti, F.; Grouve, W.J.B.; Warnet, L.L.; Villegas, I.F. Influence of Surface Preparation on Fusion Bonding of Thermoplastic Composites. In Proceedings of the 20th International Conference on Composite Materials (ICCM-20), Copenhagen, Denmark, 19–24 July 2015; Available online: https://research.utwente.nl/en/publications/influence-of-surface-preparation-on-fusion-bonding-of-thermoplast/ (accessed on 18 August 2025).
42. Wu, D.; Miao, Q.; Dai, Z.; Niu, F.; Ma, G. Effect of voids and crystallinity on the interlaminar shear strength in thermoplastic composites. *Compos. Struct.* **2022**, *300*, 114193. [CrossRef]
43. Jang, J.; Kim, H.; Park, S. Effect of Void Content on the Mechanical Properties of Composite Laminates. *Polymers* **2023**, *11*, 1251. [CrossRef]
44. Wu, Y.; Wang, K.; Neto, V.; Peng, Y.; Valente, R.; Ahzi, S. Interfacial behaviors of continuous carbon fiber reinforced polymers manufactured by fused filament fabrication: A review and prospect. *Int. J. Mater. Form.* **2022**, *15*, 18. [CrossRef]
45. Zhang, H.; Chen, J.; Yang, D. Fibre misalignment and breakage in 3D printing of continuous carbon fibre reinforced thermoplastic composites. *Addit. Manuf.* **2021**, *38*, 101775. [CrossRef]
46. Vatandaş, B.B.; Uşun, A.; Gümrük, R.; Şimşek, C. Additive manufacturing and mechanical performance of short- and continuous-fiber reinforced thermoplastic composites. *Int. J. Adv. Manuf. Technol.* **2024**, *134*, 1677–1698. [CrossRef]
47. Dankert, J.; Dankert, H. *Technische Mechanik: Statik, Festigkeitslehre, Kinematik*, 2nd ed.; Springer: Berlin, Germany, 2018.
48. Donhauser, T. Beitrag zur Auslegung hochbeanspruchter Bauteile aus Faser-Thermoplast-Verbunden. Ph.D. Thesis, Technische Universität Kaiserslautern, Kaiserslautern, Germany, 2019. Available online: https://kluedo.ub.rptu.de/frontdoor/deliver/index/docId/6083/file/Inhalt_TD-Dissertation_Druckversion-Kluedo.pdf (accessed on 18 August 2025).
49. Hashin, Z.; Rotem, A. A fatigue failure criterion for fiber-reinforced materials. *J. Compos. Mater.* **1973**, *7*, 448–464. [CrossRef]
50. A+ composites GmbH. *UD-Tape CF-PC-45-103-180: Technical Data Sheet*; A+ Composites GmbH: Gugelingen, Germany, 2024.
51. Potter, K.; Khan, B.; Wisnom, M.; Bell, T.; Stevens, J. Variability, fibre waviness and misalignment in the determination of the properties of composite materials and structures. *Compos. A Appl. Sci. Manuf.* **2008**, *39*, 1343–1354. [CrossRef]

52. Thor, M.; Sause, M.G.R.; Hinterhölzl, R.M. Mechanisms of origin and classification of out-of-plane fiber waviness in composite materials—A review. *J. Compos. Sci.* **2020**, *4*, 130. [CrossRef]
53. Thor, M.; Mandel, U.; Nagler, M.; Maier, F.; Tauchner, J.; Sause, M.G.R.; Hinterhölzl, R.M. Numerical and experimental investigation of out-of-plane fiber waviness on the mechanical properties of composite materials. *Int. J. Mater. Form.* **2021**, *14*, 19–37. [CrossRef]
54. Mehdikhani, M.; Gorbatikh, L.; Verpoest, I.; Lomov, S.V. Voids in fiber-reinforced polymer composites: A review on their formation, characterization, and mechanical effects. *J. Compos. Mater.* **2019**, *53*, 1579–1669. [CrossRef]
55. Fan, C.; Shan, Z.; Zou, G.; Zhan, L.; Yan, D. Interfacial bonding mechanism and mechanical performance of continuous fiber reinforced composites in additive manufacturing. *Chin. J. Mech. Eng.* **2021**, *34*, 21. [CrossRef]

Disclaimer/Publisher's Note: The statements, opinions and data contained in all publications are solely those of the individual author(s) and contributor(s) and not of MDPI and/or the editor(s). MDPI and/or the editor(s) disclaim responsibility for any injury to people or property resulting from any ideas, methods, instructions or products referred to in the content.